phys. stat. sol. (b) **221**, 597 (2000)

Subject classification: 61.10.Kw; 78.70.Ck

On the Theory of an X-Ray Fabry-Perot Interferometer

V. G. KOHN (a), YU. V. SHVYDKO (b), and E. GERDAU (b)

(a) Russian Research Centre "Kurchatov Institute", 123182 Moscow, Russia

(b) II. Institut für Experimentalphysik, Universität Hamburg, D-22761 Hamburg, Germany

(Received August 12, 1999; in revised form June 13, 2000)

The theory of an X-ray Fabry-Perot interferometer (FPI) is developed as a particular case of the dynamical theory of X-ray Bragg diffraction in layered crystalline systems. Mathematical expressions are derived for the transmissivity and reflectivity of the X-ray FPI built as a system of two perfect crystal plates parallel to each other. The performance of the X-ray FPI is similar to that of the optical FPI. Both show fine interference structure in the transmission and reflection dependences. However, for the X-ray FPI this occurs only inside the region of the Bragg back diffraction peak. The influence of possible imperfections, such as the roughness of the crystal plate surfaces and the error in the parallelism of the atomic planes are discussed. It is shown that both factors may significantly deteriorate the performance of the X-ray FPI. Numerical estimations are given.

1. Introduction

The Fabry-Perot interferometer (FPI) is a standard instrument for high resolution optical spectroscopy [1, 2]. Its main components are two plane mirrors of high reflectivity arranged parallel and separated by a gap. The system becomes transparent despite of the high reflectivity of each mirror when the gap d_g between the mirrors is an integer multiple of half of the radiation wavelength so that the condition for a standing wave formation in the gap is fulfilled. The free spectral range E_f, the distance between two successive transmission maxima, of a Fabry-Perot interferometer expressed on an energy (instead of the common cm^{-1}) scale is a constant independent of the photon energy and given by $E_f = hc/2d_g$. For a gap of 1 cm it amounts to 62 μeV. The spectral width Γ of the transmissivity peaks is the smaller the higher the reflectivity R of each mirror is: $\Gamma = E_f(1 - R)/\pi\sqrt{R}$. With a reflectivity of $R = 0.99$ the spectral width of the transmission lines is in the range of sub-microelectronvolts. This shows the high resolution power of an optical FPI. Such an instrument would be highly desirable also in the X-ray region. However, the optical mirrors are inefficient for X-rays.

In 1979 Steyerl and Steinhauser [3] proposed a *Fabry-Perot-type interference filter for X-rays*. They replaced the back reflection of the optical mirrors by the Bragg reflection of plane single crystal plates reflecting at a Bragg angle of precisely $\pi/2$ (back diffraction) as shown in Fig. 1. A theoretical treatment of the expected performance of the proposed instrument was given.

First experimental studies [4]–[6] of X-ray back diffraction were performed at a Bragg angle slightly less than $\pi/2$. As an exception the study [7] may be pointed out. Bragg diffraction of X-rays at normal incidence was observed only recently in single

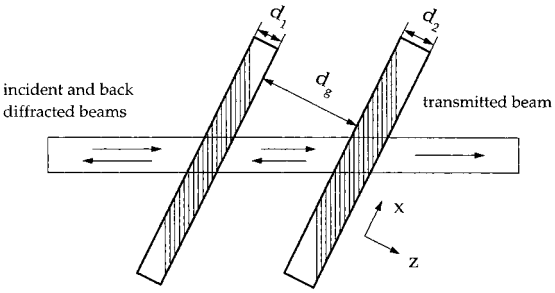

Fig. 1. Sketch of an X-ray Fabry-Perot interferometer. The mirrors are the atomic planes which are adjusted normal to the direction of the beam

crystals of silicon [8]–[11] and sapphire (Al_2O_3) [10, 12]. Back diffraction in silicon as well as in germanium, diamond, and other crystals belonging to the cubic system suffers from a fundamental drawback: it is always accompanied, except for the (111) and (220) reflections [8], by multiple Bragg diffraction [9, 10, 11, 13]. This reduces considerably the reflectivity for the back reflection channel. Sapphire does not suffer from this problem. It allows exact Bragg backscattering for X-rays of practically any energy above 10 keV by selection of the appropriate reflection and tuning the crystal temperature. As a consequence backscattering of Mössbauer radiation was observed [10, 12]. Typically Mössbauer radiation has a spectral width of a few neV, i.e., much less than the expected spectral width of transmissivity peaks of the FPI. For instance, 14.41 keV Mössbauer radiation of ^{57}Fe nuclei has a natural linewidth of 4.8 neV. To test the performance of an X-ray FPI it is thus favourable to use sapphire crystals as Bragg backscattering mirrors tuned to the energy of a Mössbauer transition. We will use the example of 14.41 keV Mössbauer radiation for numerical estimations by using the theory of an X-ray FPI presented in this paper.

The theoretical treatment of a FPI in the framework of the dynamical theory of X-ray diffraction was performed by Caticha and coauthors in a series of papers [14]–[18]. However, up to now the analysis is not complete. Especially the influence of imperfections of the FPI mirrors on the performance of the interferometer were not studied. Finally, unfortunately the analysis of the perfect FPI presented in [17, 18] contains errors.

Section 2 contains a formulation of the theory of X-ray diffraction for a perfect crystal plate at a Bragg angle of $\pi/2$. The theory is presented in a form suitable for the analysis of more complicated systems. Section 3 presents a general theory of X-ray diffraction in layered systems. The main result here will be recursion relations which allow us to calculate the parameters of scattering of the entire system from the parameters of the individual crystal plates. The theory of an X-ray Fabry-Perot interferometer is presented in Section 4. In Section 5 imperfections of the X-ray FPI such as roughness of surfaces of the FPI mirrors and misalignment of the mirrors are analyzed.

2. X-Ray Back Diffraction

Back diffraction can be treated as a special case in the general theory of Bragg diffraction [4, 16, 19, 20]. We consider the case of two-beam diffraction when the Bragg condition is satisfied only for the set of atomic planes that is represented by the reciprocal lattice vector $\mathbf{h}$. The wave vector of the incident monochromatic plane wave is $\mathbf{k}_0$. It

has the value $|\mathbf{k}_0| = K = \omega/c$ where c is the speed of light, and ω is the angular frequency. The wave vector of the diffracted wave is $\mathbf{k}_h = \mathbf{k}_0 + \mathbf{h}$. We choose the z-axis of the Cartesian coordinate system along the unit vector $\mathbf{n}$ normal to the entrance surface of the crystal plate of thickness d so that $(\mathbf{k}_0\mathbf{n}) > 0$. The vector of the electric field of the X-ray plane wave is represented as the sum of two orthogonal transverse polarization vectors: $\boldsymbol{\sigma}$ and $\boldsymbol{\pi}$. The choice of these vectors is arbitrary. In the case of exact back diffraction when $\mathbf{k}_h = -\mathbf{k}_0$, it is convenient to choose the same unit polarization vector $\mathbf{e}$ for the incident and back diffracted waves in each polarization state. With such a choice the so called "polarization factor" becomes unity for both of the polarization states. Therefore, henceforth we omit the polarization index.

For each polarization state the radiation field in the crystal may be written as a Bloch wave

$$\mathbf{E}(\mathbf{r}, t) = \exp(i\mathbf{k}_0\mathbf{r} - i\omega t)\,[E_0(z) + E_h(z)\exp(i\mathbf{hr})]\,\mathbf{e}\,. \tag{1}$$

The z dependence of the scalar amplitudes E_0 and E_h appears due to refraction at the crystal surface. In the case of a plane single crystal plate we may search the solution for the scalar amplitude as

$$E_0(z) = \sum_j \lambda_j \exp(i\varepsilon_j z)\,, \qquad E_h(z) = \sum_j \lambda_j R_j \exp(i\varepsilon_j z)\,. \tag{2}$$

The values ε and R are determined by Maxwell's equation

$$[-\mathrm{grad}^2 - K^2]\,\mathbf{E}(\mathbf{r}) = K^2\chi(\mathbf{r})\,\mathbf{E}(\mathbf{r})\,, \tag{3}$$

where $\mathbf{E}(\mathbf{r})$ is the space part of Eq. (1) and $\chi(\mathbf{r})$ is the electric part of the susceptibility of the crystal. It is a periodic function in space having the symmetry of the crystal lattice.

Substitution of Eqs. (1) and (2) in Eq. (3) and averaging over the unit cell of the crystal lattice results in

$$\begin{aligned}
&[(\mathbf{k}_0 + \varepsilon\mathbf{n})^2 - K^2] = K^2[\chi_0 + \chi_{\bar{h}}R]\,,\\
&[(\mathbf{k}_h + \varepsilon\mathbf{n})^2 - K^2]\,R = K^2[\chi_h + \chi_0 R]\,.
\end{aligned} \tag{4}$$

Here χ_0, χ_h and $\chi_{\bar{h}}$ are the Fourier components of the electric part of the susceptibility corresponding to zero, $\mathbf{h}$ and $-\mathbf{h}$ reciprocal lattice vectors, respectively. Since the interaction of X-rays with matter is weak the values of χ_0, χ_h and $\chi_{\bar{h}}$ are very small. As a result $|\varepsilon| \ll K$ and terms with ε^2 may be omitted. In this linear approximation Eqs. (4) become

$$\begin{aligned}
&2\varepsilon\gamma_0 = K[\chi_0 + \chi_{\bar{h}}R]\,,\\
&2\varepsilon\gamma_h R = K[\chi_h + (\chi_0 - \alpha)\,R]\,,
\end{aligned} \tag{5}$$

where $\alpha = (\mathbf{k}_h^2 - K^2)/K^2$ is the parameter of deviation from the Bragg condition. γ_0 and γ_h are the cosines of the angles between the normal $\mathbf{n}$ and the direction of the incident or the diffracted beam, respectively. In the case of back diffraction $\gamma_h = -\gamma_0$.

The solutions for R and ε are

$$R_{1,2} = \frac{\xi_{1,2}}{\chi_{\bar{h}}}\,, \qquad \varepsilon_{1,2} = \frac{K}{2\gamma_0}\,[\chi_0 + \xi_{1,2}]\,, \tag{6}$$

where

$$\xi_{1,2} = -y \pm \sqrt{y^2 - \chi_h \chi_{\bar{h}}}\,, \qquad y = \chi_0 - \frac{1}{2}\alpha\,. \tag{7}$$

It is assumed that the square root in Eq. (7) has a positive imaginary part.

The parameters $\lambda_{1,2}$, according to their definition in Eq. (2), are proportional to the excitation amplitude of each of the two possible waves inside the crystal. They are determined from the boundary conditions. It is assumed that at the top surface the amplitude $E_0(0)$ of the wave propagating in the direction $\mathbf{k}_0$ and at the bottom surface the amplitude $E_h(d)$ of the wave propagating in the direction $\mathbf{k}_h$ are known. Typically only one incident wave is considered by putting $E_0(0) \neq 0$ and $E_h(d) = 0$. However, if the crystal is part of a system of many parallel crystal plates (as discussed in the following sections) both amplitudes may be nonzero. By using Eq. (2) the boundary conditions are

$$\begin{aligned} &\lambda_1 + \lambda_2 = E_0(0)\,, \\ &\lambda_1 R_1\, \mathrm{e}^{i\varphi_1} + \lambda_2 R_2\, \mathrm{e}^{i\varphi_2} = E_h(d)\,, \end{aligned} \tag{8}$$

where $\varphi_{1,2} = \varepsilon_{1,2} d$. One gets

$$\lambda_1 = E_0(0) - \lambda_2\,, \qquad \lambda_2 = \frac{E_h(d) - E_0(0)\, R_1\, \mathrm{e}^{i\varphi_1}}{R_2\, \mathrm{e}^{i\varphi_2} - R_1\, \mathrm{e}^{i\varphi_1}}\,. \tag{9}$$

Equations (1), (2), (6), (7), (9) allow us to calculate the amplitudes of the radiation field at any point of the crystal. In particular for the amplitudes of the radiation field at the crystal surfaces $E_0(d)$, $E_h(0)$ using Eqs. (2), (9) one gets

$$\begin{aligned} &E_0(d) = t(d)\, E_0(0) + \bar{r}(d)\, E_h(d)\,, \\ &E_h(0) = r(d)\, E_0(0) + \bar{t}(d)\, E_h(d)\,. \end{aligned} \tag{10}$$

with

$$\begin{aligned} &t(d) = \mathrm{e}^{i\varphi_1}\, \frac{(1 - X)}{(1 - X\, \mathrm{e}^{i\varphi})}\,, \qquad \bar{t}(d) = \mathrm{e}^{-i\varphi_2}\, \frac{(1 - X)}{(1 - X\, \mathrm{e}^{i\varphi})}\,, \\ &r(d) = R_1\, \frac{(1 - \mathrm{e}^{i\varphi})}{(1 - X\, \mathrm{e}^{i\varphi})}, \qquad \bar{r}(d) = \frac{1}{R_2}\, \frac{(1 - \mathrm{e}^{i\varphi})}{(1 - X\, \mathrm{e}^{i\varphi})}\,, \\ &X = R_1/R_2, \quad \varphi = \varphi_1 - \varphi_2\,. \end{aligned} \tag{11}$$

The parameters $t(d)$ and $r(d)$ are the transmission and reflection amplitudes for the incident radiation with wave vector $\mathbf{k}_0$, and $\bar{t}(d)$ and $\bar{r}(d)$ are the transmission and reflection amplitudes for the incident radiation with wave vector $\mathbf{k}_h$.

As follows from Eq. (11), in the case of a thick crystal plate with $d \gg d_\mathrm{e}$, where $d_\mathrm{e} = \gamma_0/(K\ \mathrm{Im}\ \sqrt{y^2 - \chi_h \chi_{\bar{h}}})$ the reflection amplitude $r(d)$ does not depend on d and is equal to $r(\infty) = R_1$ with good accuracy. In this case the reflectivity becomes $P_\mathrm{r} = |r|^2$. Further on we note that in the case of vanishing absorption there is a region of total reflection with $P_\mathrm{r} = 1$ given by the condition $-|\chi_h| \leq y \leq |\chi_h|$. The phase ϕ_r of the reflection amplitude $r(\infty)$ varies in this region from $-\pi$ to 0.

We are interested in the reflectivity and transmissivity of the crystal (or crystal system) as function of energy E and angle θ between the incident X-ray beam and the

reflecting atomic planes, as well as function of temperature T. All parameters of the diffraction problem χ_0, χ_h, α depend on these variables. But the dependence of χ_0 and χ_h is very weak. They remain practically unchanged in the region of interest. By contrast the tiny variation of α in the region $|y| \leq |\chi_h|$ changes the reflectivity and the transmissivity drastically. Hence the reflectivity and the transmissivity may be expressed as function of the parameter α alone and the dependence on E, θ and T is introduced via their influence on α. In other words, only the deviation from the Bragg condition is of importance.

In the general case $\alpha(E, \theta, T)$ is given by [10, 12]

$$\alpha = 4 \frac{E_B}{E} \left[\frac{E_B}{E} - \sin\theta \right], \tag{12}$$

where $E_B(T) = hc/2d_{hkl}(T)$ is the Bragg energy for back diffraction which is determined as the energy value for $\alpha = 0$ and $\theta = \pi/2$. Here h is the Plank constant and d_{hkl} is the interplanar spacing for the reflecting planes which depends on the indices of diffraction h, k, l. Considering small deviations $\Delta E = E - E_B$, $\Delta\theta = \theta - \pi/2$ and Δd_{hkl} from the reference values E_B, $\theta = \pi/2$ and d_{hkl} in our case of back diffraction keeping the terms of lowest order we may write

$$\alpha = -4 \left(\frac{\Delta d_{hkl}}{d_{hkl}} + \frac{\Delta E}{E_B} \right) + 2 \left((\Delta\theta_x - \Delta\theta_x^{hkl})^2 + (\Delta\theta_y - \Delta\theta_y^{hkl})^2 \right). \tag{13}$$

Here $\Delta\theta_x$, $\Delta\theta_y$ describes the small angular deviations (in two independent directions) of the primary beam from normal incidence to the reflecting planes, while $\Delta\theta_x^{hkl}$, $\Delta\theta_y^{hkl}$ are the angular deviations of the reflecting planes themselves or, equivalently, the angular deviation of the reciprocal lattice vector $\mathbf{h}$ from $-\mathbf{k}_0$. These variables are convenient when one treats the diffraction problem in an imperfect crystal. One can see that both deviations may compensate each other. In the case of back diffraction the parameter α depends linearly on the variation of the X-ray energy ΔE or the interplanar distance Δd_{hkl}, however, quadratically on the angular deviation parameters.

A variation of the interplanar distance may be caused by changing the crystal temperature. In a small temperature region this variation is given with good accuracy by

$$\frac{\Delta d_{hkl}}{d_{hkl}} = C\,\Delta T, \tag{14}$$

where C is the thermal expansion coefficient. As follows from Eq. (13) the reflectivity curve on the temperature and energy scales must be the same for different angular deviations of the incident beam and only the position of the peak will be shifted by

$$\Delta T = \frac{1}{2C} (\Delta\theta)^2 \quad \text{or} \quad \Delta E = E_B \frac{(\Delta\theta)^2}{2}. \tag{15}$$

3. X-Ray Diffraction in a Layered System of Crystals

We consider plane crystal plates with each plate representing a layer of the multilayer system. It is assumed that the thickness d of the layers, the kinematical scattering amplitudes χ_0, χ_h as well as the parameter α may be different in different layers. The reflecting atomic planes of all layers, however, are taken parallel to each other. If there is a gap between successive layers filled with a non-diffracting medium, this gap will be

treated as a layer with χ_h, $\chi_{\bar{h}} = 0$. The two-beam solution of Maxwell's equation obtained in the previous section for one single crystal plate is used to calculate the reflectivity and transmissivity of the layered system. We derive recursion relations which connect the reflection $r_{\mathrm{m}}^{(k)}$ and transmission $t_{\mathrm{m}}^{(k)}$ amplitudes of a multilayer system, containing k layers, with the reflection $r_{\mathrm{m}}^{(k-1)}$ and the transmission $t_{\mathrm{m}}^{(k-1)}$ amplitudes of the first $k-1$ layers and the amplitudes r_k, t_k of the k-th layer.

We start with a system of two layers. Let the top layer have an index 1 and the parameters d_1, t_1, r_1, $\bar{t}_1$, $\bar{r}_1$, the bottom layer have an index 2 and the parameters d_2, t_2, r_2, $\bar{t}_2$, $\bar{r}_2$. The z-axis goes from top to bottom (see Fig. 2). According to Eq. (10) the following balance equations can be written for the top crystal plate:

$$\begin{aligned} E_0(d_1) &= t_1 E_0(0) + \bar{r}_1 E_h(d_1)\,, \\ E_h(0) &= r_1 E_0(0) + \bar{t}_1 E_h(d_1)\,, \end{aligned} \tag{16}$$

and for the bottom crystal plate

$$\begin{aligned} E_0(d_{\mathrm{t}}) &= t_2 E_0(d_1) + \bar{r}_2 E_h(d_{\mathrm{t}})\,, \\ E_h(d_1) &= r_2 E_0(d_1) + \bar{t}_2 E_h(d_{\mathrm{t}})\,. \end{aligned} \tag{17}$$

Here $d_{\mathrm{t}} = d_1 + d_2$ is the total thickness of the system.

We are interested in the reflection $r_{\mathrm{m}}^{(2)}$ and transmission $t_{\mathrm{m}}^{(2)}$ amplitudes of the system, which we introduce by

$$\begin{aligned} E_0(d_{\mathrm{t}}) &= t_{\mathrm{m}}^{(2)} E_0(0) + \bar{r}_{\mathrm{m}}^{(2)} E_h(d_{\mathrm{t}})\,, \\ E_h(0) &= r_{\mathrm{m}}^{(2)} E_0(0) + \bar{t}_{\mathrm{m}}^{(2)} E_h(d_{\mathrm{t}})\,. \end{aligned} \tag{18}$$

The scattering parameters are shown graphically in Fig. 2. By solving the system of Eqs. (16) and (17) one obtains the reflection and transmission amplitudes of the system as function of the reflection and transmission amplitudes of its parts,

$$\begin{aligned} t_{\mathrm{m}}^{(2)} &= \frac{t_1 t_2}{(1-\bar{r}_1 r_2)}\,, \qquad & r_{\mathrm{m}}^{(2)} &= r_1 + \frac{t_1 \bar{t}_1 r_2}{(1-\bar{r}_1 r_2)}\,, \\ \bar{t}_{\mathrm{m}}^{(2)} &= \frac{\bar{t}_1 \bar{t}_2}{(1-r_2 \bar{r}_1)}\,, \qquad & \bar{r}_{\mathrm{m}}^{(2)} &= \bar{r}_1 + \frac{t_2 \bar{t}_2 \bar{r}_1}{(1-r_2 \bar{r}_1)}\,. \end{aligned} \tag{19}$$

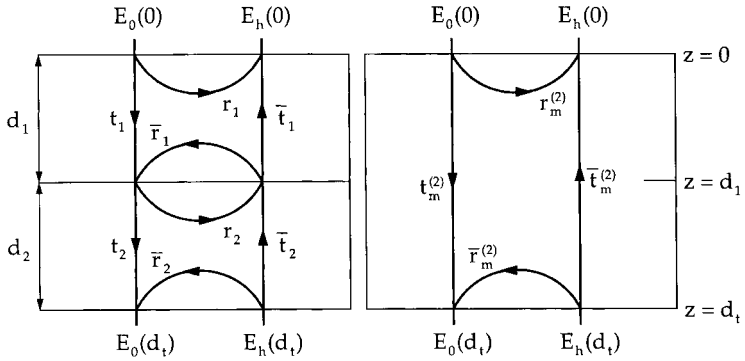

Fig. 2. Diagram showing the relation between the wave field amplitudes in a two-layer crystalline system (left) and in the complete system (right)

This solution of a two layer system allows one to give the solution of the general case of a system with k layers. We consider the top or the bottom layer of the system as a new layer added to a system containing $(k-1)$ layers. Let, for example, the bottom layer be a complex system of $(k-1)$ layers. Then $r_{\mathrm{m}}^{(2)}$ in Eq. (19) may be rewritten replacing $r_{\mathrm{m}}^{(2)}$ by $r_{\mathrm{m}}^{(k)}$, r_2 by $r_{\mathrm{m}}^{(k-1)}$ and t_1, r_1, $\bar{t}_1$, $\bar{r}_1$ by t_k, r_k, $\bar{t}_k$, $\bar{r}_k$ as

$$r_{\mathrm{m}}^{(k)} = r_k + \frac{t_k \bar{t}_k r_{\mathrm{m}}^{(k-1)}}{(1 - \bar{r}_k r_{\mathrm{m}}^{(k-1)})} \,. \tag{20}$$

One can see that in the case when the layers are numbered from bottom to top it is sufficient to consider only one recursion relation for the calculation of the reflectivity. We start with the zero value of $r_{\mathrm{m}}^{(0)}$ and successively use Eq. (20) for $k = 1, \ldots, n$ where n is the total number of layers. The recursion relation (20) for the reflectivity of a multilayer system is general and is the same in the case of grazing incidence. In a slightly different form it was proposed for the first time by Parratt [21]. For recent results on this topic see [22]–[24] and references therein.

The formula (20) can be transformed to a form, more convenient for computer calculations. By using the result of the preceding section

$$t_k \bar{t}_k - r_k \bar{r}_k = \frac{(\mathrm{e}^{i\varphi} - X)}{(1 - X\,\mathrm{e}^{i\varphi})} \tag{21}$$

one obtains after simple transformations

$$r_{\mathrm{m}}^{(k)} = \frac{R_1 - R_2 Z\,\mathrm{e}^{i\varphi}}{1 - Z\,\mathrm{e}^{i\varphi}} \,, \qquad Z = \frac{R_1 - r_{\mathrm{m}}^{(k-1)}}{R_2 - r_{\mathrm{m}}^{(k-1)}} \,. \tag{22}$$

A formula of such a type was used in [25]. In addition to the simplification of the calculation this formula uses only three parameters of each layer: R_1, R_2 and $\mathrm{e}^{i\varphi}$ instead of the four parameters of the initial recursion relation Eq. (20).

Similar to Eq. (20) one obtains the formula for the transmissivity of a system of k layers,

$$t_{\mathrm{m}}^{(k)} = \frac{t_k t_{\mathrm{m}}^{(k-1)}}{(1 - \bar{r}_k r_{\mathrm{m}}^{(k-1)})} \,. \tag{23}$$

However, it is not convenient for computer calculations. One obtains another set of equations considering the top layer as a system of $(k-1)$ layers. Then if the layers are numbered from top to bottom one gets

$$t_{\mathrm{m}}^{(k)} = \frac{t_k t_{\mathrm{m}}^{(k-1)}}{(1 - r_k \bar{r}_{\mathrm{m}}^{(k-1)})} \,, \qquad \bar{r}_{\mathrm{m}}^{(k)} = \bar{r}_k + \frac{t_k \bar{t}_k \bar{r}_{\mathrm{m}}^{(k-1)}}{(1 - r_k \bar{r}_{\mathrm{m}}^{(k-1)})} \,. \tag{24}$$

Now we may start with the values $t_{\mathrm{m}}^{(0)} = 1$, $\bar{r}_{\mathrm{m}}^{(0)} = 0$ and successively use Eq. (24) for $k = 1, \ldots, n$ where n is the total number of layers.

4. Perfect X-Ray Fabry-Perot Interferometer

The X-ray Fabry-Perot interferometer is a device which consists of two parallel crystal plates of thicknesses d_1 and d_2, separated by a gap of width d_{g} filled with a non-diffracting medium. The crystals are used as mirrors at normal incidence to the atomic planes

(see Fig. 1). It is assumed that they are made from the same material and kept at the same temperature T. The reflecting atomic planes in the second crystal plate are assumed to be perfectly parallel to the planes in the first crystal plate.

It is evident that the X-ray FPI is a particular example of a layered system discussed in the preceding section. It has three layers. The first and the third are the crystal plates, and the second is the non-diffracting medium. The position of the third layer is described by a translation vector $\mathbf{U}$. $\mathbf{U} = 0$ corresponds to a configuration where the first and the third layer are composed to a single crystal. With this choice the gap is related to $\mathbf{U}$ by $d_g = \mathbf{nU}$. To calculate the reflection and transmission amplitudes of the X-ray FPI we use the recursion relations obtained in the preceding section.

The transmission and reflection amplitudes of the first layer (first crystal mirror) are calculated by Eq. (11)

$$t_1 = t(d_1)\,, \qquad \bar{t}_1 = \bar{t}(d_1)\,, \qquad r_1 = r(d_1)\,, \qquad \bar{r}_1 = \bar{r}(d_1)\,, \tag{25}$$

and similar for the third layer (second crystal mirror)

$$\begin{aligned} &t_3 = t(d_2)\,, \qquad \bar{t}_3 = \bar{t}(d_2)\,, \\ &r_3 = r(d_2)\,\exp\,(i\mathbf{hu})\,, \qquad \bar{r}_3 = \bar{r}(d_2)\,\exp\,(-i\mathbf{hu})\,. \end{aligned} \tag{26}$$

The phase factor $\exp\,(i\mathbf{hu})$ takes into account the possible shift of the atomic planes of the second mirror relative to the planes in the first mirror. It originates from the Fourier component of the susceptibility $\chi_{\bar{h}} \to \chi_{\bar{h}}\,\exp\,(-i\mathbf{hu})$ of the second mirror. The vector $\mathbf{u} = \mathbf{U} - Nd_{hkl}\mathbf{s}_0$, where $\mathbf{s}_0 = \mathbf{k}_0/K$ and N is chosen in such a way that $\mathbf{u}$ describes a crystal lattice distortion in the second mirror (see below).

The transmissivity through the non-diffracting medium (second layer) with the electric part of the susceptibility χ_g can be easily calculated by Eq. (11) taking $\chi_0 = \chi_g$, and $\chi_h = 0$. By using these relations one obtains $\varphi_1 = K\chi_g d_g/2\gamma_0$, $\varphi_2 = K(\alpha - \chi_g)\,d_g/2\gamma_0$, and $R_1 = R_2 = X = 0$ and the transmission and reflection amplitudes for the gap read

$$t_2 = \exp\left[\frac{iKd_g}{2\gamma_0}\,\chi_g\right], \qquad \bar{t}_2 = \exp\left[\frac{iKd_g}{2\gamma_0}\,(\chi_g - \alpha)\right], \qquad r_2 = \bar{r}_2 = 0\,. \tag{27}$$

The additional phase factor $\exp\left[-iKd_g\alpha/2\gamma_0\right] = \exp\left[-id_g(k_h - k_0)/\gamma_0\right]$ in $\bar{t}_2$ appears due to different values of the wave vectors $\mathbf{k}_0$ and $\mathbf{k}_h$ if the Bragg condition is not exactly fulfilled.

Combining Eqs. (25), (26) and (27) with Eq. (19) we obtain for the reflection and transmission amplitudes of the system consisting of the second (gap) and the third (crystal) layer the expressions

$$r_m^{(2)} = r(d_2)\,\exp\,(i\phi)\,, \qquad t_m^{(2)} = t(d_2)\,\exp\,(i\varphi_g)\,, \tag{28}$$

where

$$\phi = \mathbf{hu} + 2\varphi_g - \frac{Kd_g}{2\gamma_0}\,\alpha\,, \qquad \varphi_g = \frac{Kd_g}{2\gamma_0}\,\chi_g\,. \tag{29}$$

Using Eqs. (28), (29) and the recursion relations (20), (23) one obtains the reflection and transmission amplitudes of the X-ray FPI

$$r_m = r(d_1) + \frac{t(d_1)\,\bar{t}(d_1)\,r(d_2)\,\exp\,(i\phi)}{1 - \bar{r}(d_1)\,r(d_2)\,\exp\,(i\phi)}\,, \qquad t_m = \frac{t(d_1)\,t(d_2)\,\exp\,(i\varphi_g)}{1 - \bar{r}(d_1)\,r(d_2)\,\exp\,(i\phi)} \tag{30}$$

and the reflectivity and transmissivity

$$P_{\mathrm{r}}^{\mathrm{FPI}} = |r_{\mathrm{m}}|^2 , \qquad P_{\mathrm{t}}^{\mathrm{FPI}} = |t_{\mathrm{m}}|^2 . \tag{31}$$

One may verify that for zero gap ($d_{\mathrm{g}} = 0$) in absence of the translation of the second crystal relative to the first one ($\mathbf{u} = 0$), the reflection and transmission amplitudes satisfy the obvious relation

$$t_{\mathrm{m}} = t(d_1 + d_2) , \qquad r_{\mathrm{m}} = r(d_1 + d_2) , \tag{32}$$

i.e. t_{m} and r_{m} are equal to the reflection and transmission amplitudes of a crystal with thickness $d_1 + d_2$. The same result is obtained for a nonzero gap, provided $\phi = 2\pi n$ ($n = 0, \pm 1, \ldots$) and $\chi_{\mathrm{g}} = 0$.

The formulas obtained above are similar to those of Ref. [18], however, not completely. Firstly, the formulas presented in [18] contain some misprints. Secondly, an essential α-dependence in the phase factor ϕ Eq. (29) is lacking. This leads to different properties of the X-ray FPI. Therefore, the results of computer calculations of the transmissivity obtained in [18] should be revised. It is of interest also to analyze the reflectivity of the X-ray FPI.

As an example, we present the result of a computer simulation for an X-ray FPI made of sapphire (Al_2O_3) with a vacuum gap. The sapphire crystal lattice allows two-beam back diffraction with a significant reflectivity for X-rays. We have chosen the Bragg reflection $(1\,3\,\overline{4}\,28)$ which was used in the experiment [10, 12] with $E_{\mathrm{B}} = 14.41$ keV. Figure 3 shows the energy dependence of the transmissivity for $d_1 = d_2 = 100\,\mu$m, $d_{\mathrm{g}} = 0$, 0.5, 1 mm and $s = u/d_{hkl} = 0$, 0.5. Figure 4 shows the corresponding data for the reflectivity.

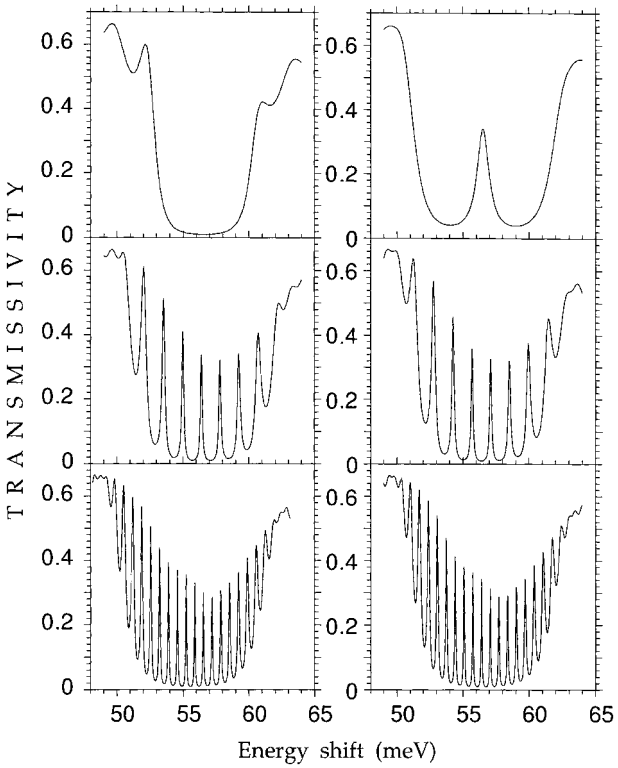

Fig. 3. Transmissivity of an X-ray Fabry-Perot interferometer as function of the X-ray energy E with respect to the Bragg energy $E_{\mathrm{B}} = 14.4125$ keV. Normal incidence is assumed to the reflecting planes $(1, 3, \overline{4}, 28)$ of sapphire (Al_2O_3) crystal plates of thickness $d_1 = d_2 = 100\,\mu$m separated by a gap of thickness $d_{\mathrm{g}} = 0$ (top), 0.5 mm (middle) and 1 mm (bottom). The relative shift of crystal lattices in the mirrors is $s = 0$ (left) and $s = 0.5$ (right)

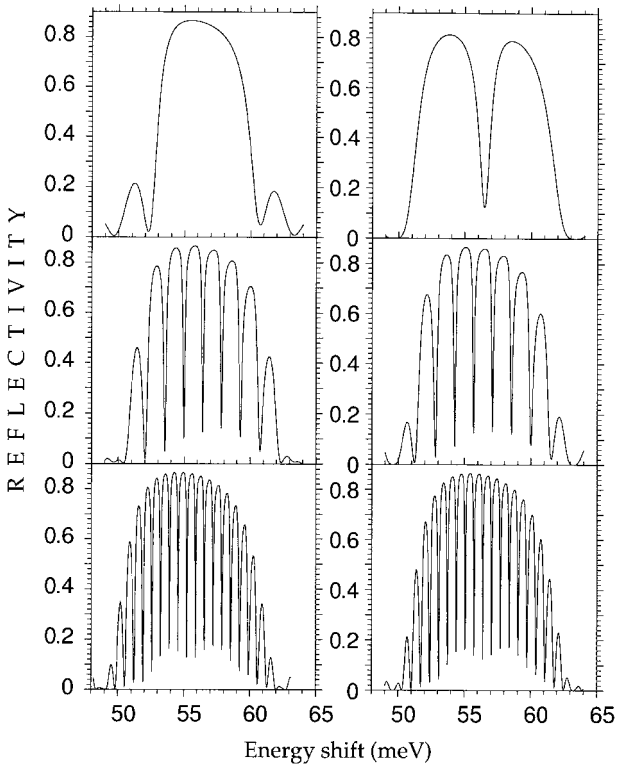

Fig. 4. Reflectivity of an X-ray Fabry-Perot interferometer with the same parameters as in Fig. 3

For zero gap the Bragg curve for backscattering is reproduced. Already a shift of the crystal lattice of one mirror relative to the other by $d_{hkl}/2$ leads to a peak of the transmissivity inside the region of high Bragg reflectivity. When the width of the gap increases more and more peaks of transmissivity arise. An additional shift of the crystal lattice of the second crystal leads to a slight shift of the transmission pattern on the energy scale. Obviously, the maxima of reflectivity coincide with pits in the transmissivity and vice versa. The sum of both curves is not unity due to absorption. The properties of a FPI well known from optics are reproduced. Additional features are due to the properties of the X-ray mirrors. One sees the well known peaks of transmissivity. The distance between them is the *free spectral range* (see Eqs. (37) and (41)). The spectral range within which transmission peaks can be observed is given by the energy width $|\chi_h|\, E_B$ of the region of total reflection.

These properties can be derived analytically from Eqs. (29) to (31). In the following analysis we assume that there is a vacuum gap between the mirrors, i.e. $\chi_g = 0$ and $\exp(i\varphi_g) = 1$. The effect of the gap reduces to the phase $\phi = \mathbf{hu} - Kd_g\alpha/2\gamma_0$.

By using Eqs. (13), (29) we have

$$\alpha = -4\left(\frac{\Delta E}{E_B} + C\,\Delta T\right) + 2(\Delta\theta)^2\,,$$

$$\phi = 2\pi\left\{s + \frac{L_g}{d_{hkl}}\left[\left(\frac{\Delta E}{E_B} + C\,\Delta T\right) - \frac{1}{2}\,(\Delta\theta)^2\right]\right\}. \tag{33}$$

Here $s = \mathbf{hu}/2\pi = u/d_{hkl}$ is the relative shift of the crystal lattices of the mirrors and $L_g = d_g/\gamma_0$ is the path length of the X-ray beam between the mirrors.

With Eq. (30), we may write the expressions for the transmissivity and the reflectivity in the form

$$P_t^{FPI} = \frac{H^2}{1 + G^2 \sin^2 [(\phi + \phi_R)/2]}, \qquad P_r^{FPI} = 1 - P_t^{FPI} - A^{FPI}, \tag{34}$$

where A^{FPI} is the amount of energy absorbed in the FPI,

$$H = \frac{T}{1 - R}, \qquad G = \frac{2\sqrt{R}}{1 - R}. \tag{35}$$

Here $T = |t(d_1)\, t(d_2)|$, $R = |\overline{r}(d_1)\, r(d_2)|$, $\phi_R = \arg [\overline{r}(d_1)\, r(d_2)]$. The formulas of Eq. (34) are similar to the Airy formulas when $T = 1 - R$ and $A^{FPI} = 0$. In optics the Airy formulas describe multiple-beam interference phenomena with two identical parallel non-absorbing mirrors of reflectivity R and thus describe also the performance of the optical FPI [1, 2]. An X-ray FPI built of identical non-absorbing crystals can be described with the same formulas as the optical FPI. The formulas of Eq. (34) have a resonance structure even in the general case of absorbing mirrors with different thicknesses.

Let us consider the energy dependence of the transmissivity of the X-ray FPI when $\Delta\theta = 0$ and $\Delta T = 0$. Within the Bragg diffraction region R is close to unity and the parameter G has a large value. In this case the transmissivity shows pronounced maxima when the condition

$$\phi = 2\pi n - \phi_R = \phi_n. \tag{36}$$

is fulfilled. Using Eq. (33) and neglecting for the moment the energy dependence of the phase ϕ_R one obtains the approximation $E_f^{(0)}$ for the free spectral range

$$E_f^{(0)} = \Delta E_n - \Delta E_{n-1} = \frac{hc}{2L_g} \approx \frac{0.620 \text{ meV mm}}{L_g}. \tag{37}$$

For values of $L_g \leq 1$ mm the spacing between the maxima of transmissivity will be small compared to the width of the Bragg diffraction region $|\chi_h|\, E_B$ which is typically 1–10 meV. In this case within the width of a separate peak of the transmissivity the parameter α varies slowly and for an approximate analysis T and R can be considered to be constant. To analyze the shape of the peak we consider a small deviation of the phase ϕ from the resonance value ϕ_n, $\phi = \phi_n + \Delta\phi$, where $|\Delta\phi| \ll 1$. We obtain a Lorentzian shape as function of $\Delta\phi$ with a maximum value of H^2 and a full width at half maximum (FWHM) of $\delta\phi = 4/G$. As in optics one can define the finesse F of the X-ray FPI as

$$F = \frac{2\pi}{\delta\phi} = \frac{\pi G}{2} = \frac{\pi\sqrt{R}}{1 - R}. \tag{38}$$

For example, $F = 29.8$ for $R = 0.9$.

The phase width $\delta\phi$ of a transmission peak can be transformed to an energy width $\Gamma^{(0)} = E_f^0/F$ taking into account the linear dependence of ϕ on ΔE, Eq. (33). If $F = 29.8$, $L_g = 1$ cm, then $E_f^{(0)} = 62$ μeV and the energy width of the transmission peak

becomes $\Gamma = 2$ μeV. It is of interest to consider also relative values

$$\frac{E_{\mathrm{f}}^{(0)}}{E_{\mathrm{B}}} = \frac{d_{hkl}}{L_{\mathrm{g}}}\,, \qquad \frac{\Gamma}{E_{\mathrm{B}}} = \frac{1}{F}\,\frac{d_{hkl}}{L_{\mathrm{g}}}\,. \tag{39}$$

The weak energy dependence of the phase ϕ_R was so far neglected in the analysis. To take it into account we consider the simple case of a crystal lattice with an inversion centre and large thickness of the mirrors $d > \gamma_0 L_{\mathrm{E}}$. Here $L_{\mathrm{E}} = 2/K|\chi_h| = 2d_{hkl}/\pi|\chi_h|$ is the extinction length in the centre of the region of total reflectivity. In this case $\phi_R = 2\phi_{\mathrm{r}}$, where $\phi_{\mathrm{r}} = \arg[r(d)]$. As pointed out in the Section 2 the phase ϕ_{r} changes from $-\pi$ to 0 within this region. Thus, there is an additional transmission peak and the real free spectral range E_{f} becomes slightly less than derived in Eq. (37) A more accurate expression for the free spectral range of an X-ray FPI can be derived.

$$E_{\mathrm{f}} = \frac{2\pi}{\partial(\phi + \phi_R)/\partial E}\,, \quad \text{where} \quad \frac{\partial\phi}{\partial E} = \frac{2\pi L_{\mathrm{g}}}{d_{hkl} E_{\mathrm{B}}}\,. \tag{40}$$

As for $\partial\phi_R/\partial E$ it is energy dependent. The mean value of $\partial\phi_R/\partial E$ can be estimated as $2\pi/|\chi_h|\,E_{\mathrm{B}}$. A detailed analytical analysis yields that in the centre of the region of total reflection the derivative is less than its mean value and equals approximately $4/|\chi_h|\,E_{\mathrm{B}}$. Since the central part of the Bragg reflectivity region is of experimental importance we use the corresponding value of $\partial\phi_R/\partial E$ for our improved estimation of the free spectral range.

$$E_{\mathrm{f}} = \frac{E_{\mathrm{f}}^{(0)}}{(1 + L_{\mathrm{E}}/L_{\mathrm{g}})}\,, \qquad L_{\mathrm{E}} = \frac{2d_{hkl}}{\pi|\chi_h|}\,, \qquad \Gamma = \frac{E_{\mathrm{f}}}{F} \tag{41}$$

This expression is similar to Eq. (20) of [18]. It is valid only within the central part of the Bragg reflection maximum. At the edges $\partial\phi_R/\partial E$ becomes strongly dependent on absorption, crystal thickness etc. and differs from the expression used. The approximation of a thick transparent mirror is no longer applicable.

We note that the values of T, R, F vary slightly inside the Bragg reflection region that leads, for example, to different heights of the peaks as seen in Fig. 3. All these features are specific to X-ray FPIs.

It is of interest to analyze the angular dependence of the transmissivity. According to Eq. (33) the phase ϕ relates quadratically to the angular deviation from normal incidence $\Delta\theta$. Therefore, the angular positions of maxima of transmissivity are not equidistant. If the X-ray energy E is chosen so, that the condition (36) is fulfilled for $\Delta\theta = 0$, then $\Delta\phi$ and $\Delta\theta$ are related by $\Delta\phi = (\pi L_{\mathrm{g}}/d_{hkl})\,(\Delta\theta)^2$ and one obtains for the FWHM of the transmission peak

$$\delta\theta = \sqrt{\frac{2d_{hkl}\,\delta\phi}{\pi L_{\mathrm{g}}}} = 2\sqrt{\frac{d_{hkl}}{L_{\mathrm{g}}F}}. \tag{42}$$

For an X-ray FPI with $L_{\mathrm{g}} = 1$ cm, $d_{hkl} = 0.43$ Å, and $F = 29.8$, the angular width of the transmission peak is $\delta\theta = 24$ μrad.

The analysis of the reflectivity of the X-ray FPI is straightforward for non-absorbing crystals. In this case $A^{\mathrm{FPI}} = 0$ and then $R^{\mathrm{FPI}} = 1 - T^{\mathrm{FPI}}$ given by Eq. (34). If $A^{\mathrm{FPI}} \neq 0$ then numerical calculations should be used for the analysis. However, in general, one

can always say that the peaks of transmissivity are accompanied by deep pits of reflectivity as seen in Fig. 4.

5. Imperfect X-Ray Fabry-Perot Interferometer

In this section we will consider the influence of possible imperfections, such as roughness of the crystal plate surfaces and the error in the parallelism of the atomic planes in the crystal plates on the performance of the X-ray FPI.

5.1 Surface roughness

5.1.1 Formulation of the approach

The roughness of the surface may be characterized by the height h of the deviation of the surface from the mean value along the surface normal and the width w of the region within the surface where h changes essentially. Due to transmission or reflection in such a spatially inhomogeneous medium the amplitude and the phase of the incident X-ray beam (the plane wave) is changed and the wave fields $E_0(z)$ and $E_h(z)$ (see Eq. (1)) become dependent on the coordinate x along the surface of the crystal in the plane of scattering. The propagation of such waves $E_0(x,z)$ and $E_h(x,z)$ in the crystal lattice is described by the two-dimensional Takagi equations [26] with spatially variable boundary conditions. We shall consider the case of back diffraction as a limit of the general case of diffraction with the Bragg angle less than $\pi/2$. As known, in a perfect crystal sample having a slightly uneven surface one may reduce the problem to an even surface and wave fields $E_0(x,0)$ and $E_h(x,0)$ at the boundary varying along the surface. The solution of the Takagi equations in this case is an integral over the line which is an intersection of the surface and the scattering plane (see, for example [27])

$$E_h(x,0) = \int_{-\infty}^{x} \mathrm{d}x'\, G_\mathrm{r}(x-x',d)\, E_0(x',0)\,,$$

$$E_0(x,d) = E_0(x_1,0) + \int_{-\infty}^{x_1} \mathrm{d}x'\, G_\mathrm{t}(x_1-x',d)\, E_0(x',0)\,, \tag{43}$$

where $x_1 = x - d/\gamma_0$, d is the crystal plate thickness. The propagators $G_s(x,d)$ $(s = r,t)$ are known analytically. They are linear combinations of Bessel functions. It is known that

$$\int_0^\infty \mathrm{d}x\, G_\mathrm{r}(x,d) = r(d)\,, \qquad 1 + \int_0^\infty \mathrm{d}x\, G_\mathrm{t}(x,d) = t(d)\,, \tag{44}$$

where $r(d)$ and $t(d)$ are defined by Eq. (11). We assume for the sake of simplicity that $E_h(x,d) = 0$.

The integral relations (43) describe the propagation of the X-ray beam in the crystal from the entrance surface to the exit surface when transmission is considered and to the entrance surface once again in the case of reflection. The propagator determines the change of the intensity and the shift of the phase of the wave field along different

trajectories. In the general case, only a finite region inside the cross section of the incident beam influences the intensity at a given point of observation at the exit surface.

In the case of back diffraction at a Bragg angle of precisely $\pi/2$, all trajectories contributing to a given point on the crystal surface reduce to the same trajectory because the trajectories of forward and back reflected rays coincide in space. This means that under the approximation discussed above we have at each spatial point of the cross section of the beam the same equations for transmissivity and reflectivity of the X-ray FPI as in the case of the perfect device. For example, for each mirror of the X-ray FPI we may use

$$E_0(x, d(x)) = t(d(x))\, E_0(x, 0) + \bar{r}(d(x))\, E_h(x, d(x))\,,$$
$$E_h(x, 0) = r(d(x))\, E_0(x, 0) + \bar{t}(d(x))\, E_h(x, d(x))\,. \tag{45}$$

Here the scattering parameters r, t, $\bar{r}$, $\bar{t}$ depend implicitly on the x coordinate along the surface by the dependence of the thickness on x. One may derive that such an approach corresponds to two-beam geometrical optics for the crystalline mirrors.

In the gap between the mirrors of X-ray FPI geometrical optics is valid when the length of transverse variation of the field is less than the region of the first Fresnel zone $\sqrt{\lambda z/\pi}$, where λ is the wavelength of X-rays and z is the path length along the beam direction. For an estimation we consider the spatial scale of transverse variation as being of the order of the length of the essential phase change due to the speed of light difference between vacuum and crystal matter, namely, $\lambda/\pi|\chi_0|$. Then we get the longitudinal distance up to which geometrical optics can be applied as $z < \lambda/\pi|\chi_0|^2$. Using the values of our example $\lambda = 0.86$ Å and $|\chi_0| = 7.8 \times 10^{-6}$ yields $z < 45$ cm. This estimation, though rather rough, shows that at least inside the entire X-ray FPI with the gap up to 1 cm geometrical optics will work well with multiple reflections when rays traverse the gap many times.

When each crystal plate has uneven surfaces one has to use local values of the thicknesses $d_1(x)$, $d_2(x)$ and $d_g(x)$, local paths of rays inside the interferometer $l_1(x)$, $l_2(x)$ and $L_g(x)$. We may apply such an approximation for the whole X-ray FPI when the width of the gap is less than 1 cm and obtain the variable transmission and the reflection amplitudes of the X-ray FPI.

The result of a measurement depends on the transverse coherence length of X-rays and the type of the detector. In the case of a coherent beam it will be different for different distances between the X-ray FPI and the position sensitive detector because the propagation of the wave through empty space is described by the Fresnel-Kirchhoff integral (Huygens-Fresnel principle). A relatively simple situation arises in the case of an incoherent beam or a short distance of the FPI to the detector with the detector having a wide window. In this case one has to average the transmissivity and reflectivity (i.e. an intensity) over the beam cross section.

Let us consider the transmissivity of an X-ray FPI under the conditions discussed above. We introduce the mean path lengths in the gap $\bar{l}_1 = \bar{d}_1/\gamma_0$, $\bar{l}_2 = \bar{d}_2/\gamma_0$ and $\bar{L}_g = \bar{d}_g/\gamma_0$ and the deviations $\Delta_1(x) = l_1(x) - \bar{l}_1$, $\Delta_2(x) = l_2(x) - \bar{l}_2$ and $\Delta_g(x) = L_g(x) - \bar{L}_g$. Now the the transmissivity per a unit length of the detector window is given by

$$\tilde{P}_t^{FPI}(\bar{d}_1, \bar{d}_2, \bar{d}_g) = \frac{1}{X} \int \mathrm{d}x\, P_t^{FPI}\big(l_1(x), l_2(x), L_g(x)\big)\,, \tag{46}$$

where X is the linear size of the surface area illuminated by the beam (the length of integration path). The dependence on x results from the parameters $\Delta_i(x)$, $i = 1, 2, g$. Since the interferometer has four surfaces there is no correlation between these random values. According to the definition of Δ we have $\overline{\Delta_1} = \overline{\Delta_2} = \overline{\Delta_g} = 0$. To satisfy these conditions we can define the mean value for each surface $\bar{s}_k$ in such a way that $\overline{(s_k(x) - \bar{s}_k)} = \overline{h_k(x)} = 0$, where $k = 1, 2, 3, 4$ denotes the surfaces numbered in the direction of the transmitted beam, then $\bar{d}_1 = \bar{s}_2 - \bar{s}_1$, $\bar{d}_g = \bar{s}_3 - \bar{s}_2$ and $\bar{d}_2 = \bar{s}_4 - \bar{s}_3$.

A similar relation applies for the reflectivity

$$\tilde{P}_t^{FPI}(\bar{d}_1, \bar{d}_2, \bar{d}_g) = \frac{1}{X} \int \mathrm{d}x \, P_r^{FPI}\big(l_1(x), l_2(x), L_g(x)\big) \,. \tag{47}$$

5.1.2 Computer simulation

An estimation of the values $\tilde{P}_t^{FPI}$ and $\tilde{P}_r^{FPI}$ may be obtained by computer simulations. The average transmissivity and reflectivity of the X-ray FPI was taken as

$$\tilde{P}_t^{FPI}(\bar{d}_1, \bar{d}_2, \bar{d}_g) = \frac{1}{N} \sum_{n=1}^{N} P_{t,r}^{FPI}(l_1^{(n)}, l_2^{(n)}, L_g^{(n)}) \,, \tag{48}$$

where $l_1^{(n)}$, $l_2^{(n)}$, $L_g^{(n)}$ are random values which were obtained from random values of the surfaces $s_j^{(n)} = \bar{s}_j + h_j^{(n)}$ as difference between two random surfaces, namely, $l_1^{(n)} = s_1^{(n)} - s_2^{(n)}$, $L_g^{(n)} = s_2^{(n)} - s_3^{(n)}$, $l_2^{(n)} = s_3^{(n)} - s_4^{(n)}$. Random values $h_j^{(n)}$ were generated in accordance with the probability distribution function $W(h)$ chosen. We start with $R = 2\,\mathrm{rnd}() - 1$, where rnd() is a random value in the interval $(0, 1)$. Then we define sign $(h) =$ sign (R), $r = |R|$ and obtain $|h(r)|$ as solution of the equation

$$r = F(|h|) = 2 \int_0^{|h|} \mathrm{d}h' \, W(h') \,. \tag{49}$$

For some simple cases of statistical distributions the dependence $|h(r)|$ can be given in analytical form. For example, for the homogeneous normalized distribution $W(h) = (2h_m)^{-1} \, \theta(h_m - |h|)$ we obtain $|h(r)| = h_m r$, where $h_m = \sqrt{3}\,\sigma$. Here and below $\sigma = \sqrt{(\overline{h^2})}$ is the rms (root mean square) value of h, $\theta(x)$ is the Heaviside step function which is unity for $x > 0$ and zero for $x < 0$. For the linear normalized distribution $W(h) = h_m^{-2} \, |h| \, \theta(h_m - |h|)$ we obtain $|h(r)| = h_m \sqrt{r}$, where $h_m = \sqrt{2}\,\sigma$. For the square normalized distribution $W(h) = 1.5 h_m^{-3} h^2 \theta(h_m - |h|)$ we have $|h(r)| = h_m r^{1/3}$, where $h_m = \sqrt{0.6}\,\sigma$. We have performed the calculations for all these distributions as well as for the Gaussian distribution $W(h) = (\sigma\sqrt{2\pi})^{-1} \exp(-h^2/2\sigma^2)$. The latter was treated numerically.

It was found that different distributions yield approximately the same results for the same rms value $\sigma = \sqrt{(\overline{h^2})}$. Figure 5 shows the results of calculations with the square distribution. We have examined a sapphire crystal at $E = 14.41$ keV. The X-ray FPI has $\bar{d}_1 = \bar{d}_2 = 100\,\mu\mathrm{m}$, $\bar{d}_g = 0.5\,\mathrm{mm}$, $\gamma_0 = 1$. The surface profiles shown at the right part of the figure were obtained after rearranging the values obtained with a random correlation length. The method is as follows. One chooses a random number of points m and puts the nearest m numbers of height h in increasing order. Then with another number of points one puts the heights in decreasing order and so on. This procedure is neces-

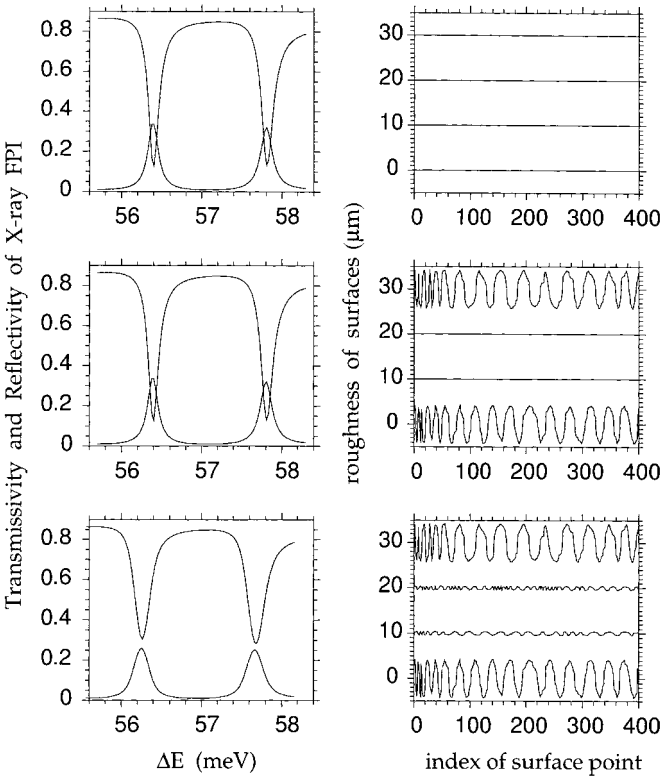

Fig. 5. Computer simulations of the influence of the surface roughness on the properties of a X-ray Fabry-Perot interferometer manufactured from sapphire crystal plates of $d_1 = d_2 = 100$ μm thickness with a vacuum gap of $d_g = 0.5$ mm. The energy of the X-rays is $E = 14.41$ keV. The left part shows the transmissivity (bottom curve) and reflectivity (top curve) of the FPI. The right part shows schematically the roughness of all surfaces of the FPI

sary only for a better view of the surface profile. The results of the calculation of transmissivity and reflectivity do not depend on the order of the random surface values.

The calculations show that the properties of the FPI are not influenced much by the roughness of the outer surfaces of the crystal mirrors in wide limits. The upper curves correspond to the case when all surfaces are even (perfect FPI). In the middle curves are given corresponding to the case when only inner surfaces are even while the outer surfaces have a roughness with a rms of $\sigma = 3$ μm. The absolute difference between top and bottom parts of the surfaces is about $2h_m = 7.5$ μm. Nevertheless, the result of the calculation shows the same peaks of transmissivity and pits of reflectivity. The bottom curves show the result of the calculation with rough inner surfaces with a rms of $\sigma = 0.25$ μm and $2h_m = 0.6$ μm. Apparently the peaks and pits begin to blur. Thus, we conclude that the roughness of the inner surfaces must be less than 0.5 μm.

5.1.3 Analytical estimations

A simple analytical estimation of the admissible roughness of the internal surfaces can be obtained. As shown in the preceding section the FWHM of the FPI resonance on

the ϕ scale is $\delta\phi = 2\pi/F = (1-R)/2\sqrt{R}$ (see Eq. (38)). We consider two values of the gap width: $d_{\rm g}^{\rm bot} = \overline{d}_{\rm g} - h_m$ and $d_{\rm g}^{\rm top} = \overline{d}_{\rm g} + h_m$. The phase difference for these two values is estimated with Eq. (33) as

$$\Delta\phi = \frac{8\pi}{\gamma_0 hc}\, h_m\, \Delta E\,, \tag{50}$$

where ΔE is the energy shift of the FPI resonance in the region of the Bragg peak relative to the Bragg energy $E_{\rm B}$. This shift of the Bragg peak is due to the different refraction coefficients in the crystal and in the gap. It can be estimated as $\Delta E = E_{\rm B}|\chi_0|/2 = hc\,|\chi_0|/4d_{hkl}$ by using Eqs. (7), (13) and taking into account that the center of the region of total reflection is at $y = 0$. The phase difference $\Delta\phi$ has to be less than $\delta\phi$ not to blur the FPI resonance. This yields

$$\frac{2h_m}{\gamma_0} = \delta L_{\rm g} < \frac{hc(1-R)}{2\pi\sqrt{R}\,\Delta E} = \frac{2d_{hkl}(1-R)}{\pi|\chi_0|\sqrt{R}}\,. \tag{51}$$

For the case considered above numerically (Al_2O_3, at $E = 14.41$ keV, $\gamma_0 = 1$, $|\chi_0| = 7.8\times10^{-6}$, $2d_{hkl} = 0.86$ Å) we have $R = 0.84$ and Eq. (51) yields $\delta L_{\rm g} < 0.6\,\mu$m. This estimation coincides rather well with the computer simulations.

5.2 Non-parallel mirrors

When the X-ray FPI is built of two separate single crystal plates the main problem is to keep the reflecting planes in different mirrors parallel. As will be shown the angle Φ which describes admissible deviations from perfect alignment is very small despite of the fact that Bragg back diffraction of a single crystal plate has a large angular width.

The error in parallelism of the atomic planes in the two crystals can be considered as a crystal lattice defect which leads to a displacement $\mathbf{u}(x,z)$ of the atoms from their ideal positions. Here we assume, as before, that the x-axis is parallel while the z-axis is normal to the surface of the crystal plate. A rotation of the crystal plate around the y-axis at the position (x_0, z_0) by a small angle Φ results in the displacement field

$$u_x = -(z - z_0)\,\Phi\,, \qquad u_z = (x - x_0)\,\Phi\,. \tag{52}$$

Such a displacement leads to an additional phase shift

$$\phi(x) = \mathbf{hu}(x) = 2\pi s(x)\,, \qquad s(x) = \gamma_0\,\frac{(x - x_0)}{d_{hkl}}\,\Phi \tag{53}$$

of the reflection amplitude of the second mirror of the X-ray FPI.

The existence of a phase shift varying in space along the surface of the X-ray FPI leads to a variation of the transmissivity. Similar to the discussion of the surface roughness we may consider each point of the surface as independent because of the validity of geometrical optics. Therefore, one has to average the transmissivity of the X-ray FPI over the the entrance window of the detector

$$\tilde{P}_{\rm t}^{\rm FPI}(d_1, d_2, d_{\rm g}) = \frac{1}{X}\int {\rm d}x\, P_{\rm t}^{X\rm FPI}\big(d_1, d_2, d_{\rm g}, \phi(x)\big)\,. \tag{54}$$

The admissible angular error of parallelism which does not destroy the peaks of transmissivity is determined by the condition $\Delta\phi < \delta\phi$, where

$$\Delta\phi = 2\pi\gamma_0\,\frac{X}{d_{hkl}}\,\Phi\,, \qquad \delta\phi = \frac{2\pi}{F} = 2\,\frac{(1-R)}{\sqrt{R}}\,. \tag{55}$$

In terms of the angle between the mirrors this means

$$\Phi < \frac{(1-R)}{\pi\gamma_0\sqrt{R}}\,\frac{d_{hkl}}{X}\,. \tag{56}$$

For $R = 0.84$, $d_{hkl} = 0.43$ Å, $X = 1$ mm one obtains $\Phi < 2 \times 10^{-9}$ rad. This is a very strong condition. It implies also that it is favourable to work with beams of small cross section.

5.3 Crystal lattice defects

The crystal lattice defects in the mirrors of the interferometer will lead to a decrease of the reflection amplitude of the X-ray mirrors as well as a partial loss of coherence of the X-ray wave. The main problem is to keep the reflection amplitude large enough because the peaks lose their sharpness when the reflectivity of the single crystal mirrors becomes small. On the other hand, even if the crystal will have a mosaic structure and different blocks of this structure will have a slightly rotated crystal lattice one may use back diffraction because it is insensitive to a rotation of the crystal lattice up to values of about $\sqrt{|\chi_h|}$. Only the size of the blocks must be larger than the extinction length. However, the extinction length increases with increasing of the local disorder and therefore a large amount of dislocations, point defects and other distortions is unacceptable.

6. Conclusion

We have analyzed theoretically the properties of an X-ray Fabry-Perot interferometer built from two perfect crystal plates parallel to each other. The arrangement is similar to the optical Fabry-Perot interferometer. However, the back reflection of the optical mirrors is replaced by the Bragg reflection of crystals reflecting at an angle of precisely 90°.

Mathematical expressions are derived for the transmissivity and reflectivity of the X-ray FPI. The performance of the X-ray FPI is similar to that of the optical FPI. Both show fine interference structure in the transmission and reflection dependences. However, for the X-ray FPI this occurs only inside the region of the Bragg back diffraction peak. Unlike the optical FPI the free spectral range turns out to be dependent on the X-ray energy.

The influence of possible imperfections, such as the roughness of the crystal plate surfaces and the error in the parallelism of the atomic planes are discussed. It is shown that both factors may significantly deteriorate the performance of the X-ray FPI. Numerical estimations are given for the case of the FPI built from sapphire (Al_2O_3) single crystals and for 14.4 keV X-rays. The admissible roughness of the inner surfaces of the crystals is about 0.5 μm. The admissible angular error in the parallelism of the atomic planes is in the nanoradian range. This renders the realization of an X-ray FPI with two independent plates more difficult.

References

[1] M. BORN and M. WOLF, Principles of Optics, Pergamon Press, Oxford 1964.
[2] J.M. VAUGHAN, The Fabry-Perot Interferometer, Hilger, Bristol 1989.
[3] A. STEYERL and K.A. STEINHAUSER, Z. Phys. B **34**, 221 (1979).
[4] W. GRAEFF and G. MATERLIK, Nucl. Instrum. and Methods **195**, 97 (1982).

[5] V.I. Kushnir and E.V. Souvorov, Zh. Eksper. Teor. Fiz., Pisma **44**, 262 (1986).
[6] R. Verbeni, F. Sette, M.H. Krisch, U. Bergmann, B. Gorges, C. Halcoussis, K. Martel, C. Masciovecchio, J.F. Ribois, G. Ruocco, and H. Sinn, J. Synchrotron Rad. **3**, 62 (1996).
[7] Yu.P. Stetsko, S.A. Kshevetskii, and I.P. Mihailiuk, Zh. Tekh. Fiz., Pisma **14**, 29 (1988).
[8] C. Cusatis, D. Udron, I. Mazzaro, C. Giles, and H. Tolentino, Acta Cryst. **A52**, 614 (1996).
[9] S. Kikuta, Y. Imai, T. Iizuka, Y. Yoda, X.-W. Zhang, and K. Hirano, J. Synchrotron Rad. **5**, 670 (1998).
[10] Yu.V. Shvydko and E. Gerdau, Hyperfine Interactions **123/124**, 741 (2000).
[11] J. Sutter, E.E. Alp, G. Bortel, M.Y. Hu, P.L. Lee, W. Sturhahn, and T.S. Toellner, to be published.
[12] Yu.V. Shvydko, E. Gerdau, J. Jäschke, O. Leupold, M. Lucht, and H.D. Rüter, Phys. Rev. B **57**, 4968 (1998).
[13] V.G. Kohn, I.V. Kohn, and E.A. Manykin, Soviet Phys. — J. Exper. Theor. Phys. **89**, 500 (1999).
[14] A. Caticha and S. Caticha-Ellis, Acta Cryst. **A37**, 267 (1981).
[15] A. Caticha and S. Caticha-Ellis, Phys. Rev. B **25**, 971 (1982).
[16] A. Caticha and S. Caticha-Ellis, phys. stat. sol. (a) **119**, 47 (1990).
[17] A. Caticha and S. Caticha-Ellis, phys. stat. sol. (a) **119**, 643 (1990).
[18] A. Caticha, K. Aliberti, and S. Caticha-Ellis, Rev. Sci. Instrum. **67**, 3380 (1996).
[19] K. Kohra and T. Matsushita, Z. Naturf. **27a**, 484 (1972).
[20] O. Brümmer, H.R. Höche, and J. Nieber, phys. stat. sol. (a) **53**, 565 (1979).
[21] L.G. Parratt, Phys. Rev. **45**, 359 (1954).
[22] W.J. Bartels, J. Hornstra, and D.J.W. Lobeek, Acta Cryst. **A42**, 539 (1986).
[23] V.G. Kohn, phys. stat. sol. (b) **187**, 61 (1995).
[24] V.G. Kohn, A.I. Chumakov, and R. Rüffer, Soviet Phys. — J. Exper. Theor. Phys. **87**, 1 (1998).
[25] M.V. Kovalchuk, V.G. Kohn, and E.F. Lobanovich, Fiz. Tverd. Tela **27**, 3379 (1985); Soviet Phys. – Solid State **27**, 2034 (1985).
[26] S. Takagi, Acta Cryst. **15**, 1311 (1962); J. Phys. Soc. Jpn. **26**, 1239 (1969).
[27] A.M. Afanasev and V.G. Kohn, Acta Cryst. **A27**, 421 (1971).